Annals of Biomedical Engineering (2023) 51:1052–1062
https://doi.org/10.1007/s10439-023-03186-1

BMES BIOMEDICAL ENGINEERING SOCIETY

ORIGINAL ARTICLE

Ventilator-Induced Lung Injury as a Dynamic Balance Between Epithelial Cell Damage and Recovery

Jason H. T. Bates[1,4] · Gary F. Nieman[2] · Michaela Kollisch-Singule[2] · Donald P. Gaver[3]

Received: 29 November 2022 / Accepted: 15 March 2023 / Published online: 31 March 2023

Abstract

Acute respiratory distress syndrome (ARDS) has a high mortality rate that is due in part to ventilator-induced lung injury (VILI). Nevertheless, the majority of patients eventually recover, which means that their innate reparative capacities eventually prevail. Since there are currently no medical therapies for ARDS, minimizing its mortality thus amounts to achieving an optimal balance between spontaneous tissue repair versus the generation of VILI. In order to understand this balance better, we developed a mathematical model of the onset and recovery of VILI that incorporates two hypotheses: (1) a novel multi-hit hypothesis of epithelial barrier failure, and (2) a previously articulated rich-get-richer hypothesis of the interaction between atelectrauma and volutrauma. Together, these concepts explain why VILI appears in a normal lung only after an initial latent period of injurious mechanical ventilation. In addition, they provide a mechanistic explanation for the observed synergy between atelectrauma and volutrauma. The model recapitulates the key features of previously published in vitro measurements of barrier function in an epithelial monolayer and in vivo measurements of lung function in mice subjected to injurious mechanical ventilation. This provides a framework for understanding the dynamic balance between factors responsible for the generation of and recovery from VILI.

Keywords Atelectrauma · Volutrauma · Multi-hit model · Rich-get-richer · Epithelial barrier dysfunction

Introduction

Up to 40% of ARDS patients lose their battle with acute respiratory distress syndrome (ARDS) [1]. While mortality from ARDS often likely reflects the inherently fatal characteristics of its underlying pathology, some patients succumb because the ongoing lung damage caused by mechanical ventilation overwhelms the innate capacity of the lung to repair itself. On the other hand, the majority of ARDS patients go on to recover, which means that the reparative capacities in these patients eventually prevail. Since there are currently no medical therapies for curing ARDS [2], minimizing its mortality amounts to achieving an optimal balance between spontaneous tissue repair versus the generation of ventilator-induced lung injury (VILI).

Although the balance between repair versus VILI remains poorly understood, we have recently obtained clues as to its general nature. Yamaguchi et al. [3] used an in vitro model of atelectrauma to show that epithelial barrier integrity initially remains normal following onset of cyclic airway recruitment and derecruitment (RD). After this initial phase, however, cell layer integrity becomes progressively diminished such that barrier-function decreases exponentially with further insult. Based on the similar well-known characteristics of cancer survival curves governed by multi-hit mechanisms [4], this leads us to hypothesize that the time-course of VILI development also reflects some kind of multi-hit process that governs the dynamics of degradation of the blood-gas barrier in the lung. In addition, Yamaguchi et al. [3] showed that the barrier integrity of an epithelial monolayer develops with

Associate Editor Chiara Bellini oversaw the review of this article.

✉ Jason H. T. Bates
jason.h.bates@med.uvm.edu

[1] Department of Medicine, University of Vermont, Burlington, VT 05405, USA

[2] Department of Surgery, SUNY Upstate Medical University, Syracuse, NY, USA

[3] Department of Biomedical Engineering, Tulane University, New Orleans, LA, USA

[4] Department of Medicine, Larner College of Medicine, 149 Beaumont Avenue, Burlington 05405-0075, USA

a characteristic time course from its initial minimum value, when the monolayer is first seeded, to its maximum value at full confluence. If we assume that the processes involved in monolayer development share many similarities to those involved in repair from physical injury, we can take the rate of development to reflect that of repair.

Based on the dynamics of barrier disruption and repair inferred from the in vitro study of Yamaguchi et al. [3], we develop in the present study a multi-hit computational model that predicts the dynamics of VILI development and resolution in the face of injurious mechanical ventilation. This model combines two levels of scale: (1) the cellular level where repetitive recruitment events impair epithelial barrier integrity by disrupting adhesions between adjacent cells and between cells and their substrates, and (2) the whole lung level where lung mechanics become deranged due to leakage of plasma fluid and proteins into the airspaces through the damaged blood-gas barrier. We show that this model potentially explains the synergy between volutrauma and atelectrauma that we have previously documented in mice [5]. We then use the model to explore some of the factors that determine whether a given regime of mechanical ventilation is injurious or safe, the goal being to develop a tool to help in the identification of ventilation strategies that permit the best chance of surviving ARDS.

Materials and Methods

We developed a computational model of VILI progression and recovery based on dynamic biophysical processes that interact across cell and organ level scales. At the level of the airway epithelial cell, biofluid mechanical stresses are hypothesized to destroy cell adhesion complexes in a stochastic manner, while spontaneous reassembly of these complexes forms the basis for recovery of epithelial barrier function. At the level of the whole lung, flux of plasma-derived fluid and proteins into the airspaces through a compromised barrier leads to the changes in lung function associated with acute lung injury. The cell and organ levels interact through the modification of the probability of disruption of cell adhesion complexes by changes in lung tissue distension during ventilation. The mathematical expression of these processes is formulated below.

Dynamics of Barrier Failure and Recovery at the Cellular Level

Yamaguchi et al. [3] simulated atelectrauma in the small airways by subjecting cultured epithelial cells in vitro to repetitive passage of an air bubble over the apical surface. The electrical impedance of the monolayer was monitored continuously as a measure of its integrity. They found that the real part of impedance, resistance (R), remained unchanged at its baseline level during passage of the first approximately 200 bubble passages across the fully confluent monolayer, after which R decreased monotonically in a quasi-exponential fashion. System evolution profiles characterized by an initial plateau that eventually transitions to a quasi-exponential decay are often governed by multi-hit processes. A classic example of this is the well-known survival probability of cancer when its pathophysiology is attributable to a multi-hit mechanism in which a number of events must occur before malignancy appears [4]. In terms of the overall shape of a multi-hit survival curve, it is not important what these events are—they can be repetitions of the same event or sequences of different events. All that matters is that they are probabilistic and statistically independent of each other. The fact that R exhibits the same overall features as seen in cancer survival curves leads us to hypothesize, by analogy, that the epithelial barrier disruption observed in the study of Yamaguchi et al. [3] was caused by the multiple hits imposed by repetitive bubble passage. This raises the question as to what is being hit. We propose that the numerous adhesion complexes that attach each epithelial cell to its neighbors and to the underlying substrate are each independent targets for the destructive effects of RD, and that barrier function itself begins to fail when enough of these adhesions have been broken.

We modeled this situation by considering a monolayer composed of N identical epithelial cells in which each cell is attached to adjacent structures (other cells and the basement membrane) by n distinct mechanical attachments each composed of one or more structural adhesions mediated by binding proteins [6]. We do not necessarily equate a cell attachment with a single protein-mediated adhesion; an attachment is simply a quantum of mechanical integrity that has some finite probability of being disrupted by bubble passage. We assume these attachments bear equal stress and contribute equally to the integrity of the monolayer. When the monolayer is fully confluent with all its attachments intact, n is at its maximum value of $n_{\max}$ and R achieves its maximum value of $R_{\max}$. Conversely, R achieves its minimum value of $R_{\min}$ when all the attachments to every cell have been disrupted such that $n = 0$. $R_{\min}$ thus represents the small but finite contribution that the fully detached cells make to the resistance of the monolayer. Since the N cells in the monolayer act in parallel to restrict the passage of electric current between the apical and basal surfaces, each cell in the monolayer has a maximum resistance of $r = R_{\max}N$ when $n = n_{\max}$, and a minimum resistance of $r = R_{\min}N$ when $n = 0$.

Each time-step in the model corresponds to a single bubble passage across the monolayer. Each such event creates a biomechanical stress on each cell that has a certain probability, p_{break}, of breaking one of its attachments (breakage

may be due to mechanical damage or active removal via some mechano-transduction mechanism [7–10]). The model is thus stochastic since, with each bubble passage, there is a probability $0 < p_{\text{break}} < 1$ that the value of n for each cell will be reduced by 1.

As the number of broken attachments, $n_{\text{broken}} = (n_{\max} - n)$, increases, we let p_{break} increase according to

$$p_{\text{break}} = \rho\left[\frac{1}{n_{\max}} + \frac{n_{\text{broken}}}{n_{\max}}\right] \tag{1}$$

where $0 \le n_{\text{broken}} < n_{\max}$ and $0 < \rho < 1$ is a constant. Since the term in the square brackets in Eq. 1 must lie between 0 and 1, this ensures that $0 < p_{\text{break}} < 1$ as must be the case if p_{break} is to be a probability. Thus, cells with fully intact attachments ($n_{\text{broken}} = 0$) have only a very small probability of $\frac{\rho}{n_{\max}}$ of experiencing an attachment break due to bubble passage, but this probability increases as attachments break. When there is only one attachment left, it has the highest probability, ρ, of breaking with the next passage. Equation 1 is in keeping with our previously articulated hypothesis that barrier failure is governed by a rich-get-richer mechanism in which large perforations in the blood-gas barrier are more likely to become further enlarged by VILI than are small perforations [11–13]. Here, we make the simple assumption that the probability of future breakage is linearly related to the number of broken attachments.

To invoke the multi-hit hypothesis, we require that a critical fraction $0 < \gamma < 1$ of the $n_{\max}$ adhesions to any given cell must be broken before that cell starts to fail in its barrier function, as reflected in a drop in r below $R_{\max}N$. Once failure begins ($n_{\text{broken}} > \gamma n_{\max}$), additional breaks cause r to drop linearly toward $R_{\min}N$. That is,

$$r = R_{\max}N \quad if \quad n_{\text{broken}} \le \gamma n_{\max} = R_{\min}N + (R_{\max} - R_{\min})N\left(\frac{n}{n_{\max} - \gamma n_{\max}}\right) \quad if \quad n_{\text{broken}} > \gamma n_{\max} = R_{\min}N \quad if \quad n = 0 \tag{2}$$

The behavior of this model of epithelial barrier disruption is thus determined by the values of the 6 parameters N, $n_{\max}$, ρ, $R_{\min}$, $R_{\max}$ and γ. We simulated this behavior with the initial condition that the value of n began as $n_{\max}$ for every cell. The effects of each subsequent bubble passage were then simulated by drawing a uniformly distributed random number x on the interval [0, 1] for each cell in turn. If $x < p_{\text{break}}$, the current value of n was decremented by 1 for the cell in question.

Yamaguchi et al. [3] also investigated the rise in R in their epithelial cell monolayer as it developed from its nascent state immediately following plating to eventually form a mature cohesive monolayer about 30 h later. The time-course of R over this period began with an initial period of about 2 h during which R was low and did not change, perhaps reflecting a period of consolidation of the plated cells before they started forming attachments. This was followed by a biphasic rise in R; the first phase was coincident with a quasi-exponential fall in monolayer capacitance, C, reflecting the strength of the cell-substrate attachments, while the second phase in R reflected the integrity of the cell–cell tight junctions [3]. We did not attempt to capture all these details in the model, but rather sought to reproduce the overall rate of rise as a global measure of epithelial repair from injury. Accordingly, we modeled formation of the monolayer by assuming that all the cell attachments are bound to their attachment sites at confluence, and that if any attachments become broken, they will reattach with a fixed probability. This means that the probability, p_{attach}, that the number of attachments to a cell will increase by 1 per unit time is proportional to n_{break} according to

$$p_{attach} = \beta n_{\text{break}} \tag{3}$$

where β is a constant. It is clear that p_{attach} must be considerably smaller than p_{break} because monolayer development takes hours to complete whereas monolayer damage takes only minutes [3]. We incorporated barrier repair into the model by, at each time step, drawing a random number x uniformly distributed on the interval [0, 1] for each cell in the epithelium in turn. If $x < p_{attach}$, we increased the current value of n for the cell in question by 1.

Dynamics of VILI Generation and Recovery at the Whole Lung Level

ARDS predisposes the lung to VILI by causing further damage to an already injured blood-gas barrier. This exacerbates the flow of fluid and proteins from the blood into the airspaces where, together with debris from local tissue damage, they interfere with surfactant function [2, 14]. Inappropriate mechanical ventilation can also directly deactivate surfactant in normal lungs without edema [15]. We previously studied this phenomenon in initially normal mice that were mechanically ventilated under anesthesia while supine with a tracheal cannula in place [5]. We found that lung over-distension (OD) alone did not cause VILI; when the animals were ventilated with PEEP = 3 cmH_2O and a large V_T commensurate with vital capacity, there was no change in lung function

over 4 h (except in those occasional cases in which a mouse developed a sudden pneumothorax). VILI was also not caused by a modest amount of RD alone, evidenced by the fact that lung function was not affected by ventilation with a modest tidal volume at zero positive end-expiratory pressure (PEEP) (under these conditions, the lungs at end-expiration were close to residual volume and thus almost certainly below closing volume [16]). This finding is supported by the study of Protti et al. [17] in pigs ventilated with low V_T at high PEEP. Interestingly, the in vitro studies described above showed that simulated RD alone is able to degrade barrier function in an epithelial monolayer. Interfacial flows likely played a key role in epithelial cell injury, as has been illustrated through in vitro [18] and in vivo [19] experiments. but the cellular stress magnitudes were likely quite different because the cultured epithelial cells were plated on a rigid substrate while the small airway epithelium in the lung is supported by structures that are compliant, particularly at low lung volumes [20]. The precise role of substrate compliance on barrier function is not entirely clear, however, since it has been shown that increased substrate compliance leads to reduced cell death while reduced compliance causes more cells to detach [21].

The key finding of our previous study in mice was that progressive VILI only occurred when OD (large V_T) and RD (zero PEEP) were present simultaneously [5]. This apparent synergy between OD and RD can potentially be explained by a rich-get-richer mechanism in which RD causes small perforations in the blood-gas barrier that are then exacerbated by OD [11]. Nevertheless, the accelerating VILI caused by simultaneous OD and RD in a normal lung only begins to manifest at about 1 h following commencement of mechanical ventilation; lung function remains normal during the first hour [5, 11, 22]. This suggests that the multi-hit phenomenon postulated above for the degradation of epithelial barrier function in vitro is also operative in vivo. We therefore propose that the synergistic effects of RD and OD cause discrete mechanical failure events in the blood-gas barrier that accumulate over time to progressively undermine its integrity. Alveolar leak and the clinical phenotype of VILI only start to appear when a certain number of failure events have occurred.

In the presence of RD, VILI is accentuated by OD in a dose-dependent manner [11, 13]. We introduce this effect into the multi-hit model developed above by having p_{break} increase with V_T through an increase in the parameter ρ in Eq. 1. Since mice do not sustain VILI when V_T is low, we assume that $\rho = 0$ when V_T is less than a critical value, V_{Tcrit}, as has been previously found in pigs [23]. We further assume that p_{break} increases asymptotically toward 1 as V_T rises above V_{Tcrit}. We represent these assumptions in the model by having ρ in Eq. 1 conform to a nonlinear expression constrained to lie between 0 and 1 thus:

$$\begin{aligned} \rho &= 0 \quad if \quad V_T < V_{Tcrit} \\ &= \frac{\left(V_T - V_{Tcrit}\right)}{\left(V_T - V_{Tcrit}\right) + A} \quad if \quad V_T \geq V_{Tcrit} \end{aligned} \tag{4}$$

where A is a constant that defines the value of V_T at which $\rho = 0.5$. Note that this scenario applies only to an initially normal lung. In a patient with ARDS, the lung is already injured and inflamed, often as a result of infection, inhalation or aspiration. While we still expect the above model to pertain in these situations, it seems very likely that the parameters defining the strength of the blood-gas barrier would need to be adjusted to reflect a greater likelihood of failure for a given level of biophysical stress.

To translate these barrier failure events into an effect on the whole lung, we need to relate them to the rate at which plasma fluid and proteins flow into and accumulate within the airspaces, labeled as (e) in Fig. 1. We model the flow of liquid into the alveolar space, $\dot{V}_{in}$, as inversely proportional to the current value of the blood-gas barrier resistance R, or $\dot{V}_{in} = B\left(\frac{1}{R}\right)$. So, as R is reduced by VILI, the rate of accumulation of liquid in the airspace increases. Likewise, we model the normal drainage of fluid from the airspaces of a healthy lung as $\dot{V}_{out} = B\left(\frac{1}{R_{max}}\right)$, where R_{max} is the barrier function of the intact monolayer. The net flow of material into the alveolar space is thus

$$\dot{V}_{net} = \dot{V}_{in} - \dot{V}_{out} = B\left(\frac{1}{R} - \frac{1}{R_{max}}\right) \tag{5}$$

where B is a constant. With damage, $R < R_{max}$, resulting in the accumulation of an excess volume, V_{excess}, of plasma-derived material in the airspaces.

In addition, there must be a mechanism for clearing this V_{excess} from the airspaces [14], otherwise there would be no possibility of eventual recovery. This clearance of plasma-derived material is labeled as (h) in Fig. 1. In the interests of keeping the model as simple as possible we assume that the rate of clearance, $\dot{V}_{clear}$, which adds to the normal rate of $\dot{V}_{out}$, is proportional to V_{excess} according to

$$\dot{V}_{clear} = k_{clear} V_{excess} \tag{6}$$

where k_{clear} is a clearance rate constant. This means that V_{excess} accrues over time according to

$$V_{excess} = \int_0^t \left[\dot{V}_{net}(t) - \dot{V}_{clear}(t)\right] dt. \tag{7}$$

Once in the airspaces, the plasma-derived material impairs pulmonary function both as a result of the fluid displacing air and the proteins inactivating pulmonary surfactant [13].

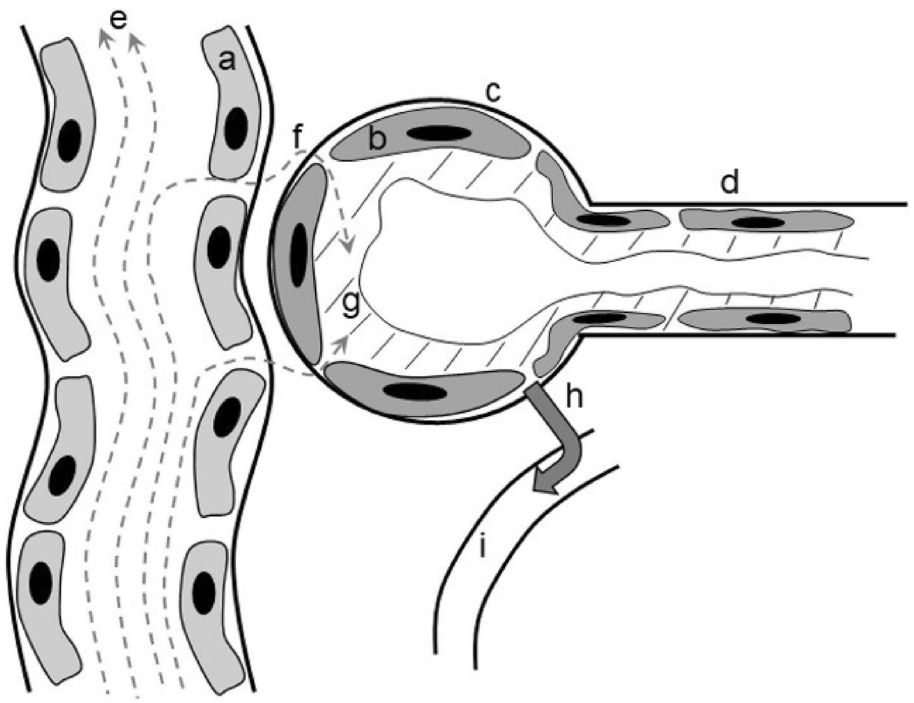

Fig. 1 Schematic of the events taking place during VILI development and resolution that are represented in the model. Endothelial cells (*a*) line a pulmonary capillary in close proximity to the epithelial cells (*b*) that line an alveolus (*c*) served by a peripheral bronchiole (*d*). Injurious mechanical ventilation causes impairment of the endothelial-epithelial barrier, as governed by Eq. 4, so that plasma fluid and proteins flowing through the capillary (*e*) leak through gaps in the blood-gas barrier (*f*) according to Eq. 5. This material accumulates in the alveolus as V_{excess} (hatched area) (*g*) according to Eq. 7, where it causes an elevation in E_{rs} according to Eq. 8. At the same time, clearance (*h*) of V_{excess} from the alveolus into the lymphatic system (*i*) leads to eventual resolution of VILI [24]

These events cause a rise in respiratory system elastance, E_{RS}, which is a key physiologic marker of VILI. While E_{RS} almost certainly increases monotonically with the accumulation of alveolar material, we do not know the precise nature of this relationship. In the interests of simplicity, we will therefore assume simple proportionality. That is,

$$E_{RS} = E_{RS,baseline} + \alpha V_{excess} \tag{8}$$

where α is a constant and $E_{RS,baseline}$ is the elastance of the uninjured respiratory system.

The complete model thus accounts for how the key biophysical mechanisms known to be behind VILI manifest in the face of the ongoing stresses wrought by mechanical ventilation. These mechanisms include the way in which physical stress causes the barrier between alveolar air and capillary blood to fail, the way in which plasma-derived material enters the airspaces as a function of barrier failure, and the counteracting mechanisms of fluid clearance that eventually lead to recovery if they are able to prevail. The behavior of complete model is determined by the values of 12 parameters that are listed in Table 1 along with their units and definitions.

Results

Figure 3 shows mean R profile ($\pm$ SD) obtained by Yamaguchi et al. [3] during formation of an epithelial monolayer. Also shown are the model predictions of barrier function obtained from Eq. 3 with $\beta = 0.01$, $R_{max} = 6 \times 10^6\ \Omega$, $R_{min} = 1 \times 10^6\ \Omega$, along with the bounding predictions obtained by varying R_{max} on either side of its aforementioned value by $2 \times 10^6\ \Omega$. The values of these three parameters are independently determined by the data in Fig. 3.

Figure 4 shows E_{RS} versus time in mice ventilated at zero PEEP with a range of large tidal volumes from 1.0 to 1.3 ml obtained from our previous study [25]. These data show an initial phase of about an hour during which E_{RS} remained essentially unchanged, followed by a monotonically increasing phase. These two phases correspond to the initial plateau phase and subsequent monotonically decreasing phase seen in R for the monolayer system (Fig. 1). Figure 4 also shows the predictions of the multi-hit computational model (Eqs. 1–8) for V_T values of 1.0, 1.1, 1.2 and 1.3 ml.

Here we used values of $N = 10,000$, $n_{max} = 25$, and $\gamma = 0.2$ as for the in vitro experiment shown in Fig. 2, while $\beta = 0.01$ as for the experiment shown in Fig. 3. We do know how R in the in vitro system relates to that in a living mouse so we normalized it for the in vivo situation such that $R_{max} = 1\ \Omega$, which then dictated that $R_{min} = 0.23\ \Omega$. The data also dictate that $E_{RS,baseline} = 23\ cmH_2O\ ml^{-1}$. The value of 0.001 min^{-1} for k_{clear} was chosen on the basis that alveolar fluid clearance has been shown to occur with a time-constant in the order of 1000 min [26]. A value for $V_{Tcrit} = 0.9$ ml was chosen on the basis that this approaches the vital capacity of a mouse, and there is evidence that the lungs may begin to experience damage when inflated repeatedly to roughly this level [5, 25]. The values of the final three parameters were determined by trial and error to

Table 1 Parameters and variables of the model

Parameter	Units	Definition
N	(none)	Number of epithelial cells in monolayer
n_{max}	(none)	Maximum number of attachments per cell
n_{broken}	(none)	Number of broken attachments to a cell
R	Ω	Resistance of monolayer
r	Ω	Resistance of single cell
R_{min}	Ω	Maximum resistance of fully intact monolayer
R_{max}	Ω	Minimum resistance of fully disrupted monolayer
γ	(none)	Fraction of cell attachments needed to maintain R_{max}
ρ	(none)	Parameter controlling probability of breakage of cell attachment
V_T	ml	Tidal volume
A	ml	Constant relating V_T and p_{break} (Eq. 4)
B	ml s^{-1} Ω^{-1}	Constant relating alveolar leak to barrier resistance (Eq. 5)
V_{Tcrit}	ml	Tidal volume threshold above which injury begins
$E_{RS,baseline}$	cmH_2O s ml^{-1}	Respiratory system elastance for an uninjured lung
α	cmH_2O s ml^{-3}	Rate at which E_{RS} increases with V_{excess} (Eq. 8)
β	(none)	Constant controlling probability of attachment
k_{clear}	min^{-1}	Rate constant of alveolar clearance of fluid and debris
$\dot{V}_{in}$	ml s^{-1}	Flow of material into airspaces
$\dot{V}_{clear}$	ml s^{-1}	Clearance flow of material from airspaces
V_{excess}	ml	Excess volume of material accumulated in airspaces

See text for the values of the parameter values used in the model simulations; these values were sometimes different between the monolayer simulation and the VILI simulation because of the different circumstances involved

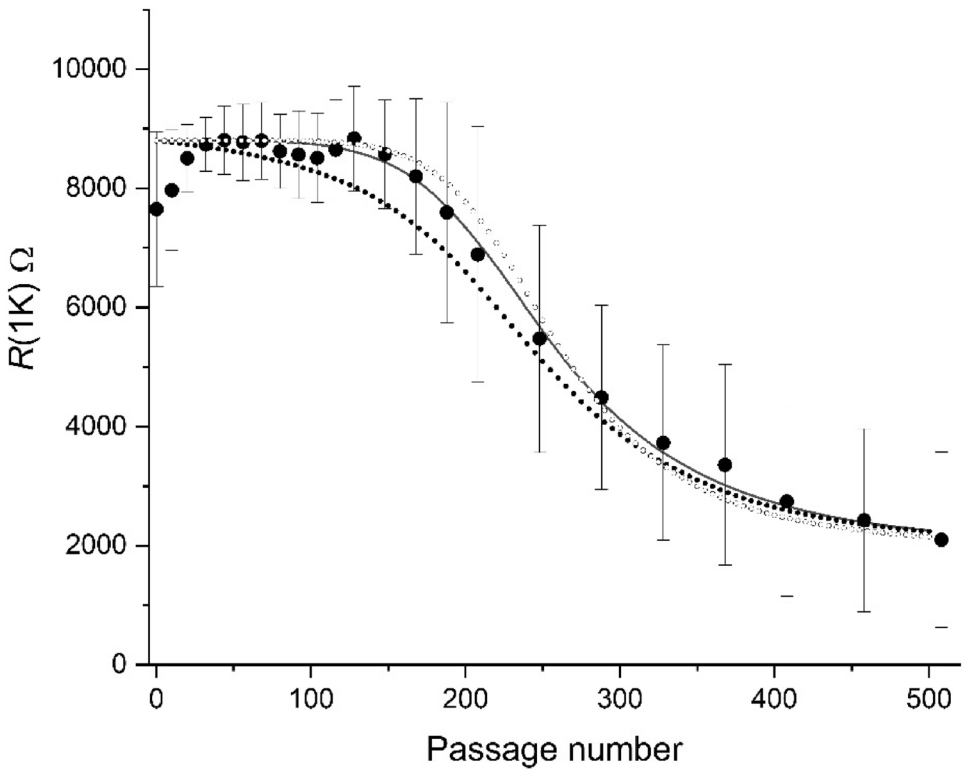

Fig. 2 Time evolution of R (mean ± SD) measured at 1 kHz (symbols, from [3]). Predictions by the stochastic model of barrier repair are shown by the solid line. The closed circles show the prediction when γ is forced to be zero. The open circles show the prediction with alternate values for n_{max} and ρ. (See text for model parameter values.)

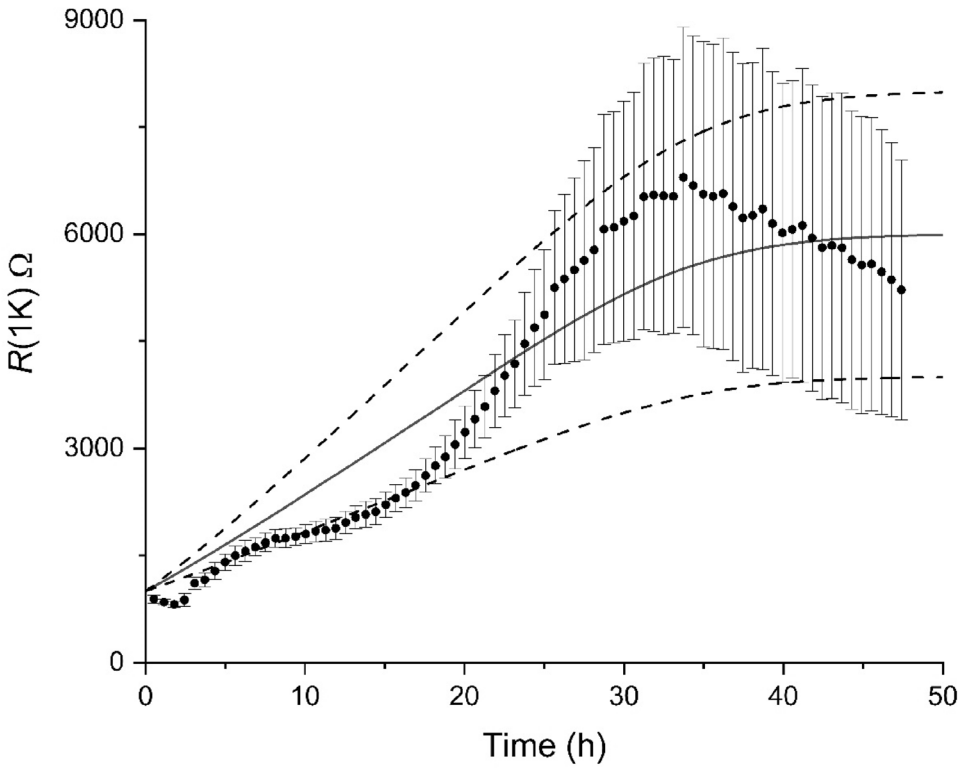

Fig. 3 Mean R ($\pm$SD) measured at 1 kHz across a cell monolayer versus the number of bubble passages forced across the layer (symbols, from [3]). Predictions by the multi-hit model of barrier disruption are shown in the solid and dashed line (see text for parameter details)

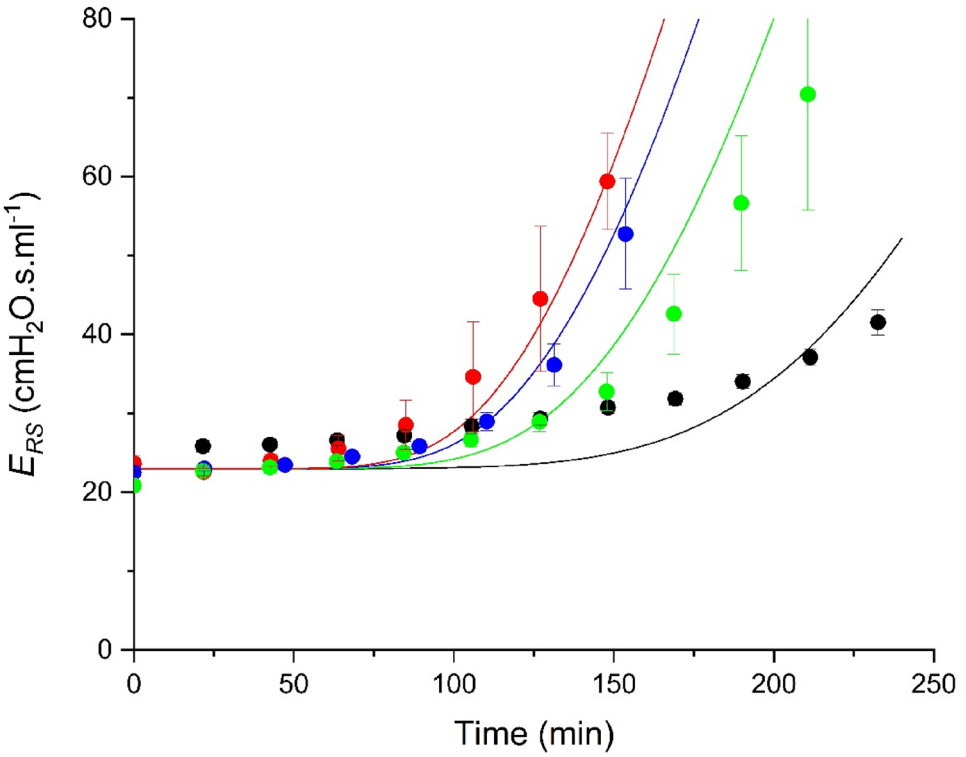

Fig. 4 Respiratory system elastance versus time in four groups of mice ventilated for 4 h at a PEEP of zero with tidal volumes ranging of 1.0 (black), 1.1 (green), 1.2 (blue) and 1.3 (red) ml. The predictions of E_{RS} by the computational model are shown as correspondingly colored solid lines (see text for parameter details)

be $A = 0.1$ ml, $B = 0.1$ ml s^{-1} Ω^{-1} and $\alpha = 1$ cmH_2O s ml^{-3}. Since the equations in which A, B and α appear (Eqs. 4, 5 and 8, respectively) represent the simplest relationships we could devise to describe the phenomena concerned, these three parameters not readily identified with any specific biophysical quantities.

The model was simulated with a time step of 1 min, so the values of p_{break} (derived from Eqs. 1 and 4) and p_{attach} corresponded to probabilities of attachment breakage and reattachment, respectively, per minute. (Here we assume that RD events take place in the lung with every breath so that a small amount of injury manifests every minute.) These model predictions recapitulate the important features of the data, particularly the delay until obvious VILI starts to occur, the rapid rise thereafter, and the increase in rate of VILI increase with increasing V_T.

Finally, we used the model to predict how VILI would progress if steps were taken to treat an already injured lung. First, we investigated the effect of instituting protective mechanical ventilation by letting VILI develop for a period of time under the same conditions as in Fig. 4 with $V_T = 1.3$ ml. Tidal volume was then suddenly reduced to a value less than V_{Tcrit} at which point, p_{break} fell immediately to zero and the lung began to heal as a result of the reestablishment of broken cell attachments governed by p_{attach}. At the same time, clearance of material from the airspaces, governed by k_{clear}, continued. Figure 5A shows the predictions of the model when V_T was reduced below V_{Tcrit} at both 120 and 150 min, the latter case allowing more injury to develop.

Interestingly, E_{RS} continued to rise in both cases for about 30 min following V_T reduction before epithelial barrier repair could bring the continued inflow of plasma-derived material under control and the alveolar clearance mechanism was able to reverse the effects of its accumulation. We also investigated the benefits of increasing V_{Tcrit} from 0.9 to 1.0 ml and of increasing k_{clear} from 0.001 to 0.002 min^{-1}. In both cases, the subsequent degree of VILI was reduced (Fig. 5B).

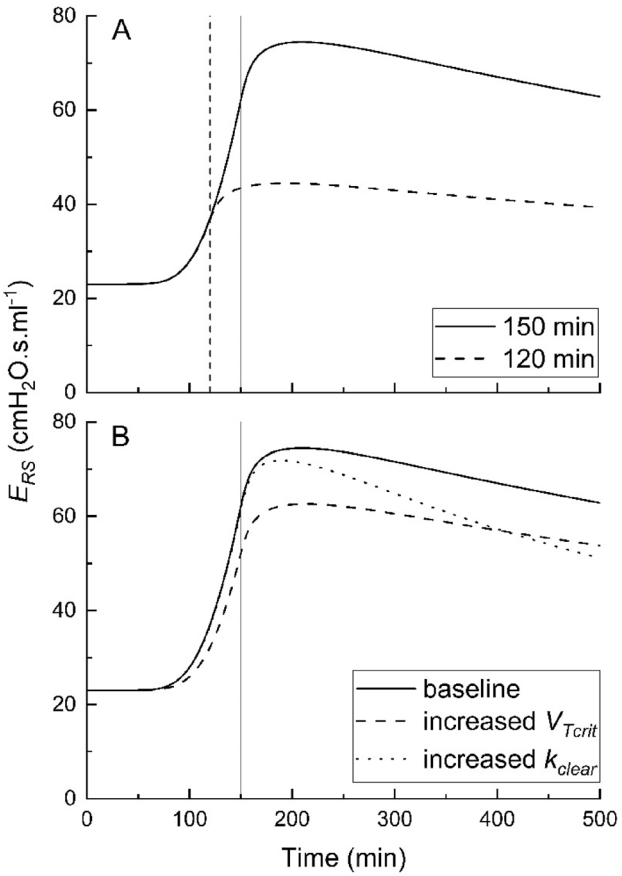

Fig. 5 E_{RS} simulated by the computational model during onset and recovery of VILI over a 500-min period of mechanical ventilation. **A** Ventilation begins with an injurious tidal volume of 1.3 ml and is then reduced below V_{Tcrit} at 120 min (dashed vertical line) and 150 min (solid vertical line). **B** Starting from a baseline condition equivalent to the solid line in **A** (solid line), V_{Tcrit} was increased from 0.9 to 1.0 ml to give the dashed line, while k_{clear} was increased from 0.001 to 0.002 min^{-1} to give the dotted line

Discussion

Volutrauma and atelectrauma have long been implicated as underlying the generation of VILI. However, while these two injury mechanisms are viewed as biophysically distinct, there is clear evidence that cyclic RD and OD interact synergistically with each other [5]. This has been explained as being due to a rich-get-richer mechanism in which initial cellular damage caused by RD is exacerbated and thus prevented by OD from spontaneously repairing itself [11, 12]. The consequence of this mechanism is that injury starts in specific regions of the lung parenchyma and then grows in both size and severity as it progresses to full-blown VILI [13]. In the present study, we propose a biophysical explanation for how this happens based on observations of the way in which epithelial barrier degradation takes place during simulated atelectrauma in vitro [3]. Borrowing from the field of cancer pathogenesis [4], the fact that barrier degradation requires a period of repetitive RD before starting to manifest, and then proceeds quasi-exponentially (Fig. 1), suggests that multiple independent events must occur before injury starts to become measurable.

We modeled this process in vitro as due to the disruption of points of physical attachment between adjacent epithelial cells in a monolayer and between the cells and their basement membrane (Fig. 1) [8–10]. Of course, the blood-gas barrier in vivo is comprised of more than just an epithelial monolayer. Therefore, to extrapolate this concept to VILI requires that it be generalized to include the degradation of whatever structural components are key in maintaining the integrity of the barrier. These additional components include

the capillary endothelium and the intervening extracellular matrix, which are anatomically in series with the alveolar epithelium. All these structures are tightly coupled structurally, however, and indeed it is clear that RD alone, which is operative only on the alveolar side of the barrier, is capable of causing alveolar leak. Accordingly, we propose that RD disrupts structures integral to the blood-gas barrier in a multi-hit fashion analogous to that described above for the epithelium in vitro. This concept suggests an explanation for the synergy between RD and OD; while it is the stresses of RD that are primarily responsible for disrupting the cell–cell and cell-substrate adhesions that maintain barrier integrity, when these adhesions are placed under additional stress by OD, their failure thresholds to RD stress are correspondingly reduced. This is represented in the model by having p_{break} increase with $V_{\mathrm{T}} > V_{\mathrm{Tcrit}}$ through Eqs. 1 and 4, and it leads to the same kind of dependence of VILI progression with V_{T} that we have previously observed in mice (Fig. 4).

At the same time, if we are to account for the fact that most ARDS patients eventually recover from the acute life-threatening stages of this often-lethal condition, it is necessary to include in the model some mechanism by which barrier function returns to normal. This repair is almost certainly a complex multi-scale process. At short timescales, for example, small tears in the epithelial cell membrane repair themselves spontaneously over minutes [27], likely representing minor damage that never becomes physiologically significant. Larger scale damage that reduces barrier function probably takes much longer to repair, the most extreme version presumably being when entire sections of epithelium are destroyed [28]. We have assumed that the dynamics of this more profound recovery is reflected in the increase in R observed during the in vitro culturing of cells, which takes place with a time-constant in the order of 20 h (Fig. 2). Accordingly, we assigned this mechanism to the spontaneous repair of disrupted cellular adhesions in our whole lung model (Fig. 4). If patients are to recover from ARDS, however, it is not enough merely to repair the barrier; the accumulation of fluid and proteins in the airspaces that is the principal cause of derangements in lung mechanics must also be cleared [24]. Alveolar fluid clearance has been shown to differ between men and women [26], and is driven to a large extent by osmotic gradients created by ion transport across the epithelium [29] and so is only fully effective when the epithelium is intact. This suggests that k_{clear} should depend on R. We do not know what this dependence should be, but our assumption that clearance is governed by a first-order mechanism (Eq. 4) is clearly an over-simplification and is meant simply to approximate the overall dynamics of the process.

The model thus recapitulates both the onset and resolution of VILI, the latter requiring the discontinuation of injurious ventilation so that the reparative processes have a chance to prevail. Obviously, the sooner this step is taken, the sooner the lung recovers (Fig. 5A). Increasing the threshold tidal volume for volutrauma, V_{Tcrit}, also decreases VILI, as does increasing the rate at which plasma-derived material is cleared from the alveolar spaces (Fig. 5B). It is not entirely clear how either of these effects might be achieved medically, but there is some evidence that stem cell therapies could help by reducing inflammation and promoting healing [30]. The model therefore provides a tool with which to investigate the conditions that lead to a favorable balance of repair over injury (in which case the patient survives), or alternatively the unfavorable conditions under which repair cannot get the upper hand (in which case the patient dies).

An interesting feature of the predictions shown in Fig. 5 is the way that injury, as reflected in E_{RS}, continues to increase for a period of time past the point at which V_{T} is reduced to a safe level. This is due to the fact that even though damage to the barrier ceases to progress when V_{T} is reduced, influx of material from the vasculature continues to accrue in the airspaces until the barrier can be repaired to the point that ongoing alveolar clearance exceeds influx of new material. Seah et al. [5] demonstrated a similar phenomenon in mice that had been ventilated with an injurious regimen to the point of having developed some degree of VILI; switching to a previously safe mode of ventilation resulted in continued VILI progression, albeit it at a slower rate. They concluded that a mechanical ventilation regimen that does not cause VILI in the normal lung may no longer be safe when applied to a lung that is already damaged. The model simulations in Fig. 5, however, suggest that this interpretation may need revision; when the originally safe regimen is re-instated, it may still be safe, but this does not manifest as an improvement in lung function until the barrier has been repaired sufficiently.

The model we have developed has a number of significant limitations largely related to its inherent assumptions, the validity of which must await the arrival of specific experimental data. We assumed that the relationships between variables such as p_{break} and V_{T} (Eqs. 1 and 4), and E_{RS} and V_{excess} (Eq. 8) are simple, that the alveolar clearance mechanism is first order (Eq. 6), and that all cells have the same maximum number of equal-strength attachments.

We further assumed that the probability of a cell attachment breaking increases in inverse proportion to the number of remaining attachments (Eq. 1). The rationale for this assumption is that the remaining attachments would have to bear the stress that was previously shared by a larger number [31], but the choice of the relationship in Eq. 1 was made purely on the grounds of simplicity; we do not know if a different relationship would be more appropriate, and indeed the data to test this possibility do not yet exist as far as we know. Our model is based on the probability of breaking a single adhesion attachment—this is simply illustrative of a

hypothesized mechanism. In fact, more than a single attachment maybe disrupted with each passage, as a function of the biomechanical stresses and the history of prior damage. Prior computational modeling suggests that when attachments break, stress on the remaining intact attachments may in some cases actually decrease [32]. We have been purposely non-specific about exactly what these attachments are comprised of, other than to suppose that they are somehow involved in the integrity of the blood-gas barrier. We also equated the rate of monolayer formation under static (non-ventilated) conditions to the rate of repair of an injured monolayer under dynamic (ventilated) conditions.

Finally, we have not built spatial heterogeneity into the model, except insofar as it arises in the course of stochastic breakage of cell attachments, because the epithelial cells are treated as all being identical. Lung injury is typically a very heterogeneous pathology, so extensions of the model could include regional variations in the number of cellular attachments and/or the probabilities that they are disrupted by RD events. For example, reopening stresses should be greater in smaller airways and alveoli following the Law of Laplace. Furthermore, surfactant deactivation caused by edema fluid entering the airspaces should increase the surface tension, which would, in turn, increase mechanical stress on airways and alveoli [33] and thus increase p_{break}.

These various assumptions were made in the interests of keeping the model as simple as possible in the absence of specific evidence to the contrary, yet they amount in many cases to little more than educated guesses, and so might best be viewed as a rationalized list of details that need to be refined through future experimentation.

In conclusion, we have developed a model of how VILI develops over time under the combined influences of atelectrauma and volutrauma. This model incorporates both our previously articulated rich-get-richer hypothesis and a new multi-hit hypothesis that explains why VILI appears in a normal lung only after there has been an initial latent period of injurious mechanical ventilation. The model recapitulates the key features of both in vitro measurements of epithelial monolayer barrier function and in vivo measurements of lung function. The numerous assumptions made in constructing the model present targets for further investigation toward a more detailed understanding of the factors responsible for the generation of and recovery from VILI.

Acknowledgements This work was supported by NIH Grant HL142702 and W81XWH-20-1-0696.

Author Contributions Study concept and design: JHTB. Drafting of Manuscript: JHTB. Critical Revisions of Manuscript: DPG, MK-S, GFN. Statistical Analysis: JHTB. Obtaining Funding: GFN, DPG, JHTB.

Funding Funding was provided by Center for Scientific Review (Grant No. HL142702).

Declarations

Competing Interests JHTB is a member of the advisory board and shareholder in Oscillavent, LLC. He is also a consultant for Respirator Sciences LLC and is co-applicant on patent Application WO2015127377 A1 (filed Feb 23, 2014) and International application no. PCT/US21/24537 (filed March 2, 2021). GFN has an Unconditional Education Grant from Drager Medical. GFN and MKS have lectured for Intensive Care On-line Network, Inc. (ICON). MKS has received an educational research grant from Dräger Medical Systems, Inc. The authors maintain that industry had no role in the design and conduct of the study; the collection, management, analysis, or interpretation of the data; nor the preparation, review, or approval of the manuscript.

References

1. Bellani, G., J. G. Laffey, T. Pham, E. Fan, L. Brochard, et al. Epidemiology, patterns of care, and mortality for patients with acute respiratory distress syndrome in intensive care units in 50 countries. *JAMA*. 315:788–800, 2016.
2. Matthay, M. A., R. L. Zemans, G. A. Zimmerman, Y. M. Arabi, J. R. Beitler, et al. Acute respiratory distress syndrome. *Nat. Rev. Dis. Primers*. 5:18, 2019.
3. Yamaguchi, E., J. Yao, A. Aymond, D. B. Chrisey, G. F. Nieman, et al. Electric cell-substrate impedance sensing (ECIS) as a platform for evaluating barrier-function susceptibility and damage from pulmonary atelectrauma. *Biosensors (Basel)*. 12:390, 2022.
4. Atwood, K. C., and A. Norman. On the interpretation of multi-hit survival curves. *Proc. Natl. Acad. Sci. USA*. 35:696–709, 1949.
5. Seah, A. S., K. A. Grant, M. Aliyeva, G. B. Allen, and J. H. Bates. Quantifying the roles of tidal volume and PEEP in the pathogenesis of ventilator-induced lung injury. *Ann. Biomed. Eng.* 39:1505–1516, 2011.
6. Jacob, A. M., and D. P. Gaver 3rd. Atelectrauma disrupts pulmonary epithelial barrier integrity and alters the distribution of tight junction proteins ZO-1 and claudin 4. *J. Appl. Physiol.* 1985(113):1377–1387, 2012.
7. Moriondo, A., P. Pelosi, A. Passi, M. Viola, C. Marcozzi, et al. Proteoglycan fragmentation and respiratory mechanics in mechanically ventilated healthy rats. *J. Appl. Physiol.* 1985(103):747–756, 2007.
8. Pelosi, P., and P. R. Rocco. Effects of mechanical ventilation on the extracellular matrix. *Intensive Care Med.* 34:631–639, 2008.
9. Novak, C., M. N. Ballinger, and S. Ghadiali. Mechanobiology of pulmonary diseases: a review of engineering tools to understand lung mechanotransduction. *J. Biomech. Eng.* 2021. https://doi.org/10.1115/1.4051118.
10. Han, B., M. Lodyga, and M. Liu. Ventilator-induced lung injury: role of protein-protein interaction in mechanosensation. *Proc. Am. Thorac. Soc.* 2:181–187, 2005.
11. Hamlington, K. L., J. H. T. Bates, G. S. Roy, A. J. Julianelle, C. Charlebois, et al. Alveolar leak develops by a rich-get-richer process in ventilator-induced lung injury. *PLoS ONE*. 13:e0193934, 2018.
12. Mori, V., B. J. Smith, B. Suki, and J. H. T. Bates. Linking physiological biomarkers of ventilator-induced lung injury to a rich-get-richer mechanism of injury progression. *Ann. Biomed. Eng.* 47:638–645, 2019.
13. Gaver, D. P., 3rd., G. F. Nieman, L. A. Gatto, M. Cereda, N. M. Habashi, and J. H. T. Bates. The POOR Get POORer: a hypothesis for the pathogenesis of ventilator-induced lung injury. *Am. J. Respir. Crit. Care Med.* 202:1081–1087, 2020.

14. Beretta, E., F. Romano, G. Sancini, J. B. Grotberg, G. F. Nieman, and G. Miserocchi. Pulmonary interstitial matrix and lung fluid balance from normal to the acutely injured lung. *Front Physiol.* 12:781874, 2021.
15. Albert, R. K. The role of ventilation-induced surfactant dysfunction and atelectasis in causing acute respiratory distress syndrome. *Am. J. Respir. Crit. Care Med.* 185:702–708, 2012.
16. Gomes, R. F., X. Shen, R. Ramchandani, R. S. Tepper, and J. H. Bates. Comparative respiratory system mechanics in rodents. *J. Appl. Physiol.* 1985(89):908–916, 2000.
17. Protti, A., D. T. Andreis, G. E. Iapichino, M. Monti, B. Comini, et al. High positive end-expiratory pressure: only a dam against oedema formation? *Crit. Care*. 17:R131, 2013.
18. Bilek, A. M., K. C. Dee, and D. P. Gaver 3rd. Mechanisms of surface-tension-induced epithelial cell damage in a model of pulmonary airway reopening. *J. Appl. Physiol.* 1985(94):770–783, 2003.
19. Hussein, O., B. Walters, R. Stroetz, P. Valencia, D. McCall, and R. D. Hubmayr. Biophysical determinants of alveolar epithelial plasma membrane wounding associated with mechanical ventilation. *Am. J. Physiol. Lung Cell Mol. Physiol.* 305:L478–L484, 2013.
20. Gaver, D. P., D. Halpern, O. E. Jensen, and J. B. Grotberg. The steady motion of a semi-infinite bubble through a flexible-walled channel. *J. Fluid Mech.* 319:25–65, 1996.
21. Higuita-Castro, N., C. Mihai, D. J. Hansford, and S. N. Ghadiali. Influence of airway wall compliance on epithelial cell injury and adhesion during interfacial flows. *J. Appl. Physiol.* 1985(117):1231–1242, 2014.
22. Smith, B. J., E. Bartolak-Suki, B. Suki, G. S. Roy, K. L. Hamlington, et al. Linking ventilator injury-induced leak across the blood-gas barrier to derangements in murine lung function. *Front Physiol.* 8:466, 2017.
23. Protti, A., M. Cressoni, A. Santini, T. Langer, C. Mietto, et al. Lung stress and strain during mechanical ventilation: any safe threshold? *Am. J. Respir. Crit. Care Med.* 183:1354–1362, 2011.
24. Matthay, M. A. Resolution of pulmonary edema. Thirty years of progress. *Am. J. Respir. Crit. Care Med.* 189:1301–1308, 2014.
25. Smith, B. J., K. A. Grant, and J. H. Bates. Linking the development of ventilator-induced injury to mechanical function in the lung. *Ann. Biomed. Eng.* 41:527–536, 2013.
26. Bastarache, J. A., T. Ong, M. A. Matthay, and L. B. Ware. Alveolar fluid clearance is faster in women with acute lung injury compared to men. *J. Crit. Care*. 26:249–256, 2011.
27. Gajic, O., J. Lee, C. H. Doerr, J. C. Berrios, J. L. Myers, and R. D. Hubmayr. Ventilator-induced cell wounding and repair in the intact lung. *Am. J. Respir. Crit. Care Med.* 167:1057–1063, 2003.
28. Gill, S. E., C. M. Yamashita, and R. A. Veldhuizen. Lung remodeling associated with recovery from acute lung injury. *Cell Tissue Res.* 367:495–509, 2017.
29. Folkesson, H. G., and M. A. Matthay. Alveolar epithelial ion and fluid transport: recent progress. *Am. J. Respir. Cell Mol. Biol.* 35:10–19, 2006.
30. Zanirati, G., L. Provenzi, L. L. Libermann, S. C. Bizotto, I. M. Ghilardi, et al. Stem cell-based therapy for COVID-19 and ARDS: a systematic review. *NPJ Regen. Med.* 6:73, 2021.
31. Gattinoni, L., E. Carlesso, P. Cadringher, F. Valenza, F. Vagginelli, and D. Chiumello. Physical and biological triggers of ventilator-induced lung injury and its prevention. *Eur. Respir. J. Suppl.* 47:15s–25s, 2003.
32. Hamlington, K. L., B. Ma, B. J. Smith, and J. H. Bates. Modeling the progression of epithelial leak caused by overdistension. *Cell Mol. Bioeng.* 9:151–161, 2016.
33. Ghadiali, S., and D. P. Gaver. The influence of non-equilibrium surfactant dynamics on the flow of a semi-infinite bubble in a rigid cylindrical capillary tube. *J. Fluid Mech.* 478:165–196, 2003.